

Experimental Analysis and Optimization of Process Parameters on Weld Characteristics of SS 410 Using TIG Welding

¹Dr. P. Hema, ²M. Vinay Kumar, ³U. Sainadh

^{*1}Assistant Professor, Department of Mechanical Engineering, SVUCE, Tirupati – 517 502

^{*2}PG Student, Department of Mechanical Engineering, SVUCE, Tirupati – 517 502

^{*3}Academic Consultant, Department of Mechanical Engineering, SVUCE, Tirupati – 517 502

Corresponding Author: ¹Dr. P. Hema

ABSTRACT

The main aim of the current investigation is to optimise the process parameters and the effect of the welding characteristics of grade 410 stainless steel welding joints by Tungsten Inert Gas (TIG) welding process. The consistency of the welding bead is also dictated by its geometry and configuration, which in turn, is affected by different control variables, such as the peak current, the base current and gas pressure of the welding process. Experiments are carried out by Gray Relation Analysis (GRA) based on a Taguchi design of experiment and optimization. Data from the tests are obtained and performance responses such as Hardness and Impact Strength are analyzed. For smaller hardness and greater impact strength by Taguchi using the MINITAB programming, ideal execution parameters are found. The effect of TIG process parameters is measured using ANOVA and S/N ratios of robust nature, and the optimal welding state is calculated to optimize the mechanical properties of the joint. An attempt is made using NDT-Magnetic Particle Tester to examine and measure the TIG welded joints.

KEYWORDS: Tungsten Inert Gas (TIG) welding, Hardness, Impact Strength, Taguchi Design, Gray Relation Analysis (GRA), ANOVA, NDT – Magnetic Particle Tester.

Date of Submission: 18-11-2020

Date of acceptance: 03-12-2020

I. INTRODUCTION

Welding is a permanent bonding procedure used by applying heat and or pressure to bind various materials such as metals, alloys or plastics together on their contact surfaces. The workpieces to be joined are melted at the interface during the welding process and a permanent joint can be obtained after solidification. In order to form a welding pool of molten material that provides a tight bond between the materials after solidification, a filler material is also applied. Material weldability depends on numerous variables, such as the metallurgical modifications that arise during welding, changes in weld zone toughness due to rapid solidification, the degree of oxidation due to atmospheric oxygen reaction of materials and the propensity to develop cracks in the joint location.

1.1 TIG Welding Mechanism

TIG welding is an arc welding process that uses a non-consumable tungsten electrode to create the weld. The welding area is shielded by an inert shielding gas (argon or helium) from the atmosphere and a filler metal is usually used. The electricity is supplied from a welding torch from the power source (rectifier), which is transmitted to a tungsten electrode that is fitted into the handpiece. An electric arc is then generated between the tungsten electrode and the workpiece by a column of strongly ionized gas and metal vapours using a constant-current welding power supply that produces energy which is carried out through the arc. Tungsten electrodes and the welding field are shielded by inert gas from the ambient air. Temperatures of up to 20,000⁰C can be created by the electric arc and this heat can be concentrated on melting and joining two distinct material components. It can use the weld pool with or without filler material to connect the base metal. Figure 1 displays a graphical diagram of the principle of TIG welding.

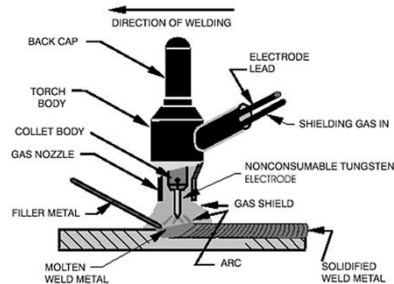


Figure 1: Principle of TIG Welding

II. LITERATURE REVIEW

TIG welding is a highly accurate and unpolluted welding process, but it is very important to monitor and attain various welding parameters for a good outcome. The operator selects the multiple welding parameters depending on his knowledge or from a literature survey.

L. Suresh Kumar et.al [1], have studied the welding features of AISI 410 and 316 austenitic stainless steel alloys for MIG and TIG welding processes and the ideal welding properties of the metals have also been established.

Almazrouee et.al[2] investigated the influence of the parameters of welding on the low alloy steel welding bead geometry using the Flux-Cored Arc Welding Process (FCAW). Built models are tested for their validity and relevance and further validated using additional experimental verification results.

Sudakaran. R et.al [3], analyzed the influence of the Gas Tungsten Arc Welding (GTAW) parameters on the pitting corrosion on AISI 202 chromium manganese stainless steel. An empirical mathematical equation was developed correlating the equal number of pitting resistance (PREN) with welding parameters such as welding current, welding speed, welding gun angle, and gas flow rate. The core composite surface response technique, with four parameters and five stages, is used to execute the trials. The adequacy of the built model has been tested using ANOVA. The efficiency of the welding joint is also greatly determined by the microstructure of the welding.

T. A. Tabish et.al [4], investigated the effect of heat input on the microstructure and mechanical properties of welded joints of AISI 410 stainless steel TIG. The method is applied by differing heat inputs (low, medium and high) to various specimens. It explores the welded joints' microstructural features and mechanical properties. The findings found that the tensile strength of welded samples is greater than that of the base metal.

Benjamin Joseph [5] studied the welding metal characterization of 316L (N) austenitic stainless steel by the electron beam welding process by adjusting the welding parameters such as beam strength and welding speed. The studies are carried out by studying the welded material's mechanical and metallurgical properties. In compliance with ASTM standards, the mechanical properties were measured using tensile, impact, hardness and bending measurements.

In order to describe the microstructure of Alloy 690-SUS 410L stainless steel, **J. L. Jeng [6]** carries out dissimilar welds with Inconel 52 and 82 filler metals (I-52 and I-82). For gas tungsten arc welding, the welds are butt-welded. Microstructural tests are carried out from the centre of each fusion zone on the samples prepared. TiN_s are found in the inter-dendritic region and along the grain boundaries of the I-52 fusion zone, while Ti-Nb-rich phases were found in the I-82 fusion zone. In the root regions of both I-52 and I-82 welds, the grain boundary content of Cr was greater than 9 percent.

Jun Yan[7] studied various welding methods, such as Tungsten Inert Gas (TIG) welding, laser welding and laser-TIG combination welding, and analysed the microstructure and mechanical properties of 410 stainless steel joints. To examine the phase composition, X-ray diffraction is used, while microscopy is done to study the microstructure properties of joints. Tensile experiments are eventually undertaken and the fracturing surfaces are examined. The findings showed that in all joints, the joint by laser welding had the maximum tensile strength and the smallest dendrite size, while the joint by TIG welding had the lowest tensile strength and the largest dendrite size. The observation of the fractograph shows that the TIG welding joint existed as a cup-cone shaped fracture, while the laser welding and composite welding joints existed as pure shear fracture. Because of their high welding speed and outstanding mechanical properties, laser welding and hybrid welding are ideal for welding 410 stainless steel.

Radha Raman Mishra[8] researched Tungsten Inert Gas (TIG) and Metal Inert Gas (MIG) welding processes for stainless steel grades 202, 410, 310 and 316 with mild steel. The percentage of joint dilutions is measured and the tensile strength of the dissimilar metal joints is tested. For various joints made by TIG and

MIG welding processes, the findings are compared and it has been found that TIG welded dissimilar metal joints have stronger physical properties than MIG welded joints.

K. Monika et.al [9],has studied the effect of heat input on the mechanical properties of dissimilar MIG welded joints.Gas Metal Arc Welding prepares two dissimilar joints (IS2062-IS 45 C8) and (IS2062-IS 103 Cr 1) and observes mechanical properties.The input is taken into account in his work under two conditions. i) low heat input dissimilar joints i.e. in IS 2062-IS 45 C8 (3,6189 kj/mm) and IS 2062-IS 103 Cr 1 (4,01973 kj/mm) ii) high heat dissimilar joints i.e. in IS 2062-IS 45 C8 (3,1421 kj/mm) and IS 2062-IS 103 Cr 1 (3,70537 kj/mm)are taken and the mechanical properties are studied and finally compared with the heat input suitable for dissimilar joints for the current working conditions.

Raveendra A et.al [10],have investigated the effect of fusing parameters on the weld bead geometry such as front width and back width of weld joint on 5052 aluminium alloy sheet. Welding current, gas flow rate and welding speed are taken into account during experimental work and found increase in heat energy on workpiece surface by increasing the welding current which results as increasing the front width and back width of weld joint linearly. Front width and back width of weld joint decreases linearly with the increment of welding speed. Front width and back width of weld joint increases or decreases alternatively with increasing of gas flow rate.

2.1 Objectives of the Present Work:

The main objective of this work is to get the minimum changes in the physical properties and no metallurgical defect during welding process. Based on the objective, the scope of the work consists of:

- To conduct the experiments using TIG welding process of SS 410 alloy pieces with non- consumable electrode.
- Find out the output responses like Impact strength and Hardness of those pieces.
- Conducting the experiments as per the Taguchi L9 orthogonal array and find out the responses, S/N Ratios and Analysis Variance.
- Optimization of the process parameters on output responses using Grey Relational Analysis.
- NDT – Magnetic Particle Test has been conducted on SS 410 weld alloy pieces to evaluate the welding defects, discontinuities and breakages without causing damage to the original part.

III. METHODOLOGY

Taguchi's strategy is an effective method for the plan of a brilliant framework. It gives, a productive as well as an orderly way to deal with improve plans for execution and quality. Moreover, Taguchi parameter configuration can lessen the change of framework execution. The experiment is governed by the following steps are:

- **Process parameters selection:** Process parameters and their ranges are determined by the research work.The parameters are identified for the joining of SS 410 metals are Peak Current, Base Current and Gas Pressure.
- **Orthogonal array selection:** To select an appropriate orthogonal array for the experiments, on the basis of parameter selection and its levels. Here, three parameters and three levels are selected. The control factors and their levels are shown in Table 1.

Table 1: Control Factors and their Levels

Control Factors	Level 1	Level 2	Level 3
Peak Current (Amps)	160	180	200
Base Current (Amps)	20	30	40
Gas Pressure (Kg/mm ²)	4	5	6

The control parameters thought to have significant effects on the quality characteristic. Control parameters are those design factors that can be set and maintained. The levels for each test parameter must be chosen at this point. The number of levels, with associated test values, for each test parameter defines the experimental region.

- **Conduct the experiments:** Nine experimental runs are conducted as per the Taguchi's L9 orthogonal array. The test runs are carried out at random to avoid a systematic error creeping into the experimental procedure.
- **Grey Taguchi Technique:** The analysis of performance parameters can be obtained by using Grey Relation Grade (GRG). This analysis is employed to find the optimal performance parameter levels and to analyze the influence of these parameters on Hardness and Impact Strength.

IV. EXPERIMENTAL SETUP AND EXPERIMENTATION

4.1 Experimental Setup:

Unitor UWI 400 Power Source and an automated welding set up is chosen for the conducting of experiments. In this welding machine automated Tungsten Inert Gas torches as well as automatic feeler wire feeding units are considered for welding of SS 410 workpieces. The experimental setup and specifications of TIG welding machine is shown in Figure 2 and Table 2. The welding setup consists of different parts:

- **TIG welding torch** –With the movable tractor unit, the Torch is fixed. In the torch, a tungsten electrode is fixed and Argon gas flows through it.
- **TIG welding machine** –This is the key component of the TIG welding method that supplies regulated amounts of current and voltage during welding. A rectifier was used with a current range of 10-180 A and a voltage of up to 230 V, depending on the current environment.
- **Gas cylinder** –Argon gas is supplied to the welding torch with a specific flow rate for TIG welding to form an inert atmosphere and create a steady arc for welding. The flow of gas is regulated by regulators and valves.
- **Work holding table** –In order to hold the work piece, a surface plate (made of grey cast iron) is used to preserve the welding distance between the tungsten electrode and the workpiece. In order to keep the piece of work, proper clamping was used.
- The torch is kept at an angle of about 90 ° from the workpiece.



Figure 2: TIG Welding Machine Setup

Table 2: Specifications of TIG Welding Machine

Amps	20 -300/TIG
TIG	16 Amps /415v
Cooling	Air cooling
Frequency	50Hz
Filler Rod	ER 410
Shielding Gas	Pure Argon

4.2 Base Material (Workpiece):

Primarily stainless steel is categorised into various groups such as austenitic, ferrite, martensitic etc. I have picked martensitic stainless steel (410) from this because of its low cost, convenient consumer usability that is the kind of stainless steel which is commonly used. It has a chromium content of at least 12 percent, which creates the steel structure completely martensitic and offers ductility, a broad duty temperature scale, non-magnetic properties and strong potential for welding. Due to its many benefits and fast market availability, stainless steel is chosen for transport out of the experimental study.

SS410 is a martensitic stainless steel that offers strong resistance to corrosion plus high strength and hardness. In both the annealed and hardened cases, it is magnetic. With various heat treatments, a broad range of properties can be produced. For this alloy, applications requiring mild corrosion resistance and high mechanical characteristics are desirable. Flat springs, knives, cooking utensils and hand tools are common applications.

In this work, SS 410 10 mm thick martensitic stainless steel samples were welded to each other using a 1.2 mm diameter welding wire using the semi-automated Gas metal arc welding process. Table 3 and Table 4 show the chemical structure of SS 410 and the mechanical properties of grade 410 stainless steel.

Table 3: Chemical Composition of 410 Grade Stainless Steel

SS410Grade	C%	Mn%	Si%	P%	S%	Cr%
	0.15	1.0	1.0	0.04	0.030	11.5 – 13.5

Table 4: Mechanical Properties of 410 Grade Stainless Steel

Mechanical Properties	Values
Density (Kg/m ³)	7.7x10 ³
Poisson's Ratio	0.27 – 0.30
Elastic Modulus (GPa)	160 – 200
Tensile Strength (Mpa)	517
Yield Strength (Mpa)	265
Elongation (%)	30

4.3 Experimental Procedure

Workpieces are butted around a longitudinal segment and rigidly mounted using clamps on the dense backing plate, which is mechanically fixed. Initially the parameters considered for experimentation are peak current, base current and gas pressure. The experiments are conducted for the peak current range of 160 A to 200 Amps, base current ranging from 20 to 30 Amps and gas pressure ranging from 4 to 6 Kg/mm². The corresponding welded joints images of the SS 410 workpieces are shown in Figure 3.

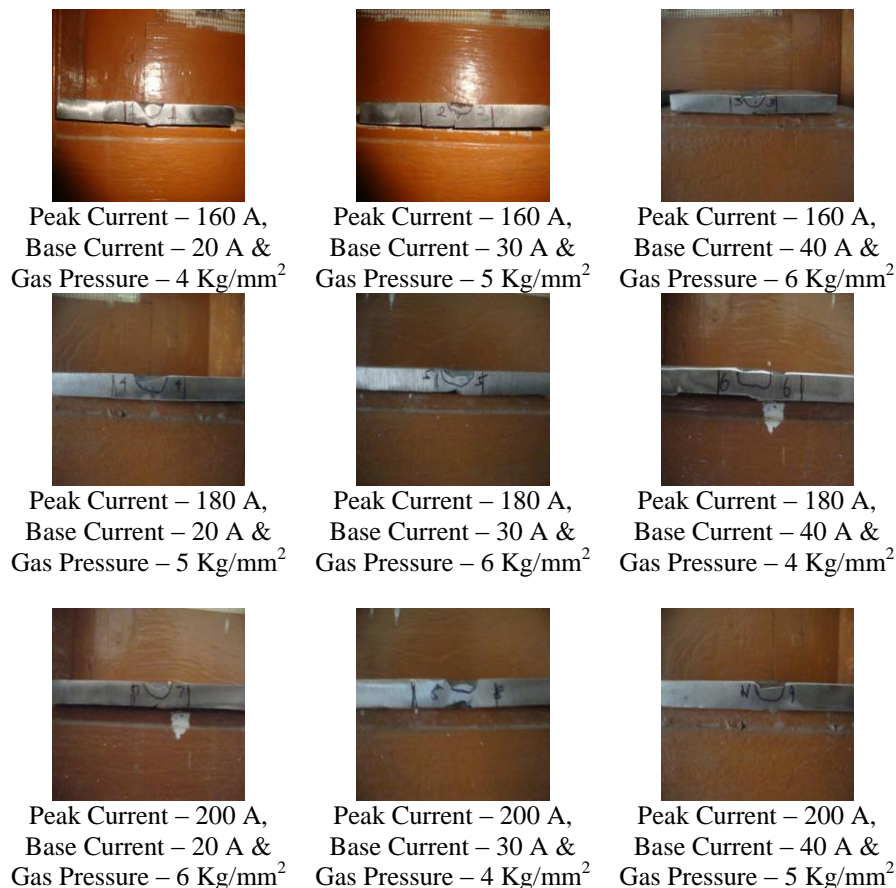


Figure 3: Images of the TIG welded Workpieces

4.4 Hardness Test:

Hardness devices use a direct reading machine that calculates the hardness amount based on either a diamond point or a steel ball's penetration distance. A substance having a low Rockwell Hardness number was shown by deep penetration. A limited penetration, however, suggests a substance with a high level of Rockwell hardness. "The number of Rockwell hardness is based on the difference in the depth to which a penetrator is driven by a definite load of light or "minor" and a definite load of heavy or "major. The ball penetrators are chucks which are made to accommodate reinforced steel balls of 1/16" or 1/8" diameter. 1/4" and 1/2" ball penetrators for the testing of softer materials are also available. There are two kinds of anvils on the Rockwell hardness testers that are used. For flat specimens, the Flat Faceplate versions are used. Anvils of the "V" type carry round specimens securely. Flat steel or brass blocks, which have been checked and labelled with the scale and Rockwell number, are test blocks or calibration blocks. They can be used to periodically validate the tester's precision and calibration. In Figure 4, the photos of the hardness test specimens are shown.



Figure 4: Hardness Test for L9 Specimens

4.5 Impact Tests:

Charpy impact testing method is used for impact test of SS 410 welded specimens. In power generation markets, this method is utilized in such services as mechanical testing. In our implementation of Charpy impact test, specimens are cut from metal samples, and a V-notch is placed in the center. Charpy impact testing can be performed at ambient and low temperatures (down to -325°F). Three Charpy test specimens are assessed, often in accordance with the ASTM standards. The corresponding test specimen images are shown in Figure 5.



Figure 5: Impact tests pieces of L9 specimens

The responses for the hardness and impact test of SS 410 workpieces are shown in Table 5.

Table 5: L9 Orthogonal Array with responses of Impact Strength and Hardness

S. No.	Peak Current (amp)	Base Current (amp)	Gas Pressure (kg/mm ²)	Impact Strength (kn/mm ²)	Hardness
1	160	20	4	38	88
2	160	30	5	44	86
3	160	40	6	32	92
4	180	20	5	36	98
5	180	30	6	38	93
6	180	40	4	40	94
7	200	20	6	38	85
8	200	30	4	42	95
9	200	40	5	26	87

4.6 Optimization of Process Parameters:

Grey Relational Analysis (GRA) has a wide area of application in manufacturing processes. This approach can solve multi-response optimization problem simultaneously planning the experiments through the Taguchi orthogonal array has been used quite successfully in process optimization.

GRA involves pre-processing stages wherein the output parameters are normalized. Normalization is a very important step in GRA. The reason is that GRA is a multi-objective optimization technique and depends on more than one parameter for its result. The output parameters being analyzed normally are of different units. During normalization, all the output parameters are converted into dimensionless values.

The formulas for the normalization process are as follows

$$\text{Nominal the better, } Y(k) = 1 - \frac{|x_i^o(k) - x^o|}{\max x_i^o(k) - x_i^o(k)}$$

$$\text{Smaller the better, } Y(k) = \frac{\max x_i^o(k) - x_i^o(k)}{\max x_i^o(k) - \min x_i^o(k)}$$

$$\text{Higher the better, } Y(k) = \frac{x_i^o(k) - \min x_i^o(k)}{\max x_i^o(k) - \min x_i^o(k)}$$

where, $Y(k)$ = The normalized value for the k^{th} trial

$x_i^o(k)$ = The value of the output parameter for the k^{th} trial

$\min x_i^o(k)$ = The smallest value of the output parameter "x" for the k^{th} trial

$\max x_i^o(k)$ = The largest value of the output parameter "x" for the k^{th} trial

The next step is the calculation of the Grey Relation Co-efficient (GRC). The GRC for any output parameter can be calculated using the formula,

$$\eta(j) = \frac{\Delta_{\min} + \zeta \Delta_{\max}}{\Delta_{oi} + \zeta \Delta_{\max}}$$

where, $\eta(j)$ = GRC for the j^{th} output parameter

$$\Delta_{oi} = \left| |x_o^*(k) - x_i^o(k)| \right| = \text{Deviation Sequence}$$

$x_o^*(k)$ = Reference Sequence

$$\Delta_{\min} = \min \left| |x_o^*(k) - x_i^o(k)| \right|$$

$$\Delta_{\max} = \max \left| |x_o^*(k) - x_i^o(k)| \right|$$

ζ = weighting coefficient

The weighting coefficient indicates the importance of the output parameter. The output parameters can be weighted by giving suitable values to the weighting coefficient. However, if all the output parameters are of equal importance the value of the weighting coefficient is taken as "0.5". Thus the GRC is calculated for each of the output parameters. The closer the value is to "1", the better is its performance, i.e., it satisfies the conditions of higher/lower to greater extent.

Calculation of the GRG is the final step in GRA. Though, secondary analysis exists after this step, the actual GRA ends with this step. GRG is the step where the optimization technique converts from a single objective optimization to a multi-objective optimization. The GRG is calculated as an average of the GRCs of all the output parameters at a given level of the OA. The formula for GRG is

$$\text{GRG} = \frac{1}{n} \sum_{j=1}^n \eta(j)$$

Where n = number of output parameters

According to the Taguchi method, if the effects of the control factors on performance are additive, it is possible to predict the performance for a combination of levels of the control factors by knowing only the main effects of the control factor.

V. RESULTS AND DISCUSION

5.1 Optimization Using Grey Taguchi Method:

The grey relation analysis is carried out for the optimum parameters and corresponding values are shown in Table 6 for optimization of processes parameters.

Table 6: Grey Relational Analysis

Exp. No.	Grey Relation Generation		Grey Relation Coefficient		GRG
	Impact Strength	Hardness	Impact Strength	Hardness	

1	0.667	0.769	0.600	0.684	0.642
2	1.000	0.923	1.000	0.867	0.933
3	0.333	0.462	0.429	0.481	0.455
4	0.556	0.000	0.529	0.333	0.431
5	0.667	0.385	0.600	0.448	0.524
6	0.778	0.308	0.692	0.419	0.556
7	0.667	1.000	0.600	1.000	0.800
8	0.889	0.231	0.818	0.394	0.606
9	0.000	0.846	0.333	0.765	0.549

5.2 Characteristic Curves for Hardness:

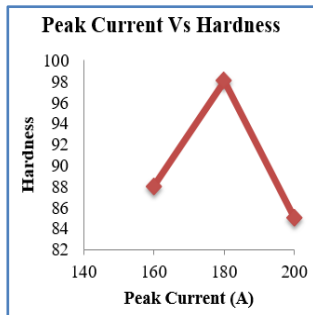


Figure 6 (a): Peak Current Vs Hardness

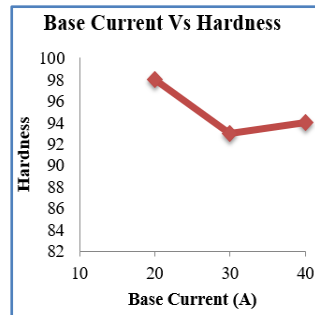


Figure 6 (b): Base Current Vs Hardness

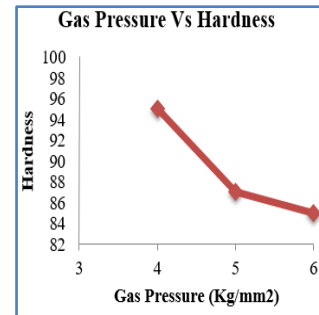


Figure 6 (c): Gas Pressure Vs Hardness

From Figures 6 (a), 6 (b) and 6(c), it is observed that

- **Peak Current Vs Hardness:** Hardness is increasing from 86 to 98 with increasing peak current from 160 A to 180 A and then decreasing from 98 to 84 with increasing 180 A to 200 A.
- **Base Current Vs Hardness:** Hardness is decreasing from 98 to 93 with increasing base current from 20 A to 30 A and then slightly increasing from 93 to 94 with increasing 30 A to 40 A.
- **Gas Pressure Vs Hardness:** Hardness is decreasing from 95 to 87 with increasing gas pressure from 4 to 5 Kg/mm² and then decreasing from 87 to 85 with increasing 5 to 6 Kg/mm².

5.3 Characteristic Curves for Impact Strength:

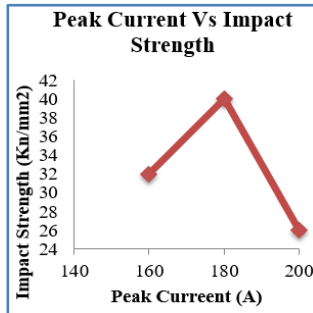


Figure 7 (a): Peak Current Vs Impact Strength

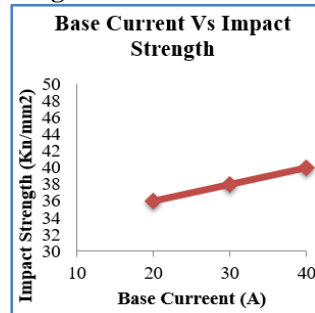


Figure 7 (b): Base Current Vs Impact Strength

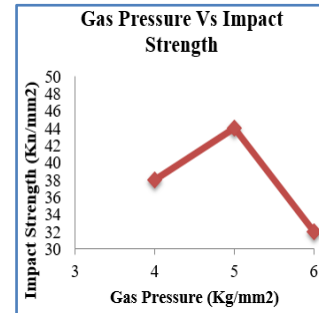


Figure 7 (c): Gas Pressure Vs Impact Strength

From Figures 7 (a), 7 (b) and 7 (c), it is observed that

- **Peak Current Vs Impact Strength:** Impact Strength is increasing from 32 to 40 with increasing peak current from 160 A to 180 A and then decreasing from 40 to 26 with increasing 180 A to 200 A.
- **Base Current Vs Impact Strength:** Impact Strength is increasing from 36 to 38 with increasing base current from 20 A to 30 A and then gradually increasing from 38 to 40 with increasing 30 A to 40 A.
- **Gas Pressure Vs Impact Strength:** Impact Strength is increasing from 38 to 42 with increasing gas pressure from 4 to 5 Kg/mm² and then decreasing from 42 to 32 with increasing 5 to 6 Kg/mm².

The Main Effects plot for GRG is obtained for set of experiments gives optimal process parameters by using MINITAB R16 software.

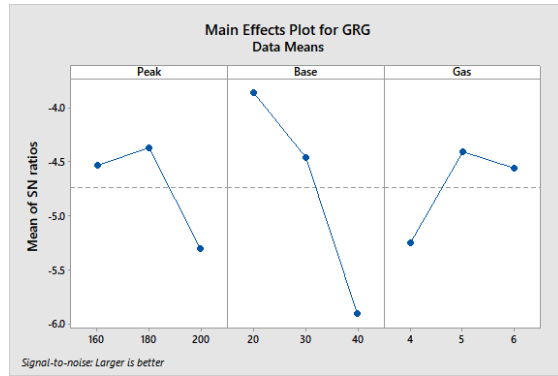


Figure 8: Main effects plot for S/N ratios of GRG

From the Figure 8, it can be observed that the optimum input parameters at maximum GRG are peak current (180 A), base current (20 A) and gas pressure (5 Kg/mm²).

5.4 Analysis of Variance (ANOVA):

A mathematical approach for evaluating the presence of variations between many means of population is the Study of Variation (ANOVA). While the purpose of ANOVA is to discern variations between means of multiple populations, the procedure involves the study of various types of variance correlated with the random samples being tested, hence the term analysis of variance analysis.

Table 7: Analysis of Variance for Hardness

Source	DF	Seq SS	Adj SS	F	P	% of contribution
Peak Current	2	76.222	38.1111	0.98	0.504	46
Base Current	2	1.556	0.7778	0.02	0.980	1
Gas Pressure	2	9.556	4.7778	0.12	0.890	6
Error	2	77.556	38.7778			47
Total	8	164.889				100

From Table 7, it is observed that the % contribution of values for hardness at peak current (46), base current (1) and gas pressure (6). It is observed that the peak current have great influence on hardness. Since this analysis is a parameter based optimization design, from the above values it is clear that gas pressure is the major factor to be selected effectively to get the good hardness.

Table 8: Analysis of Variance for Impact Strength

Source	DF	Seq SS	Adj SS	F	P	% of Contribution
Peak Current	2	14.22	7.111	0.21	0.826	6
Base Current	2	112.89	56.444	1.67	0.374	49
Gas Pressure	2	38.22	19.111	0.57	0.639	16
Error	2	67.56	33.778			29
Total	8	232.89				100

From Table 8, it is observed that the % contribution of values for impact strength at peak current (6), base current (49) and gas pressure (16). It is observed that the base current have great influence on impact strength. Since this analysis is a parameter based optimization design, from the above values it is clear that base current is the major factor to be selected effectively to get the maximum impact strength.

5.5 Non Destructive Testing (Magnetic Particle Testing):

Table 9: NDT (Magnetic Particle Testing) Values of SS 410

Specimen No.	Peak Current(amps)	Base Current(amps)	Indications	Result
1	160	20	NI	Accepted
2	160	30	NI	Accepted
3	160	40	UC	Rejected
4	180	20	NI	Accepted
5	180	30	NI	Accepted
6	180	40	NI	Accepted
7	200	20	NI	Accepted
8	200	30	Por	Accepted
9	200	40	CR	Rejected

Where, NI –No Indications, CR – Crack, UC – Undercut and Por – Porosity

From Table 9, it is seen that out of 9 weld specimens only two specimens are rejected and remaining 7 no's are welded joints are accepted by the NDT tester (Magnetic Particle Tester). It is observed that the weld joints for suitable fabrication purposes.

VI. CONCLUSIONS

- The SS 410 specimens are joined by using TIG welding machine upon changing different control factors like peak current, base current and gas pressure.
- The optimum process parameters obtained for multi response optimization through GRG technique are Peak Current 160 A, Base Current 30 A, and Gas Pressure 5 Kg/mm²
- The % contribution of values for hardness at peak current (46), base current (1) and gas pressure (6). It is observed that the peak current have great influence on hardness. Since this analysis is a parameter based optimization design, from the above values it is clear that gas pressure is the major factor to be selected effectively to get the good hardness.
- The % contribution of values for impact strength at peak current (6), base current (49) and gas pressure (16). It is observed that the base current have great influence on impact strength. Since this analysis is a parameter based optimization design, from the above values it is clear that base current is the major factor to be selected effectively to get the maximum impact strength.
- The TIG welded joints exhibited better mechanical and metallurgical characteristics with 90 – 95% of parent material's Hardness value.
- The specimen failures are associated depending upon the improper changes of heat value and it creates so many metallurgical defects and it is identified by using NDT testing.
- From NDT – Magnetic particle tester, out of 9 specimens only 2 specimens are rejected and remaining 7 specimens are accepted for joining of metal by TIG welding machine.

REFERENCES

- [1]. Mr.L.Suresh Kumar, Dr.T.SivaShankar, "Experimental Investigation for Welding Aspects of AISI 410& 316 by Taguchi Technique for the Process of TIG & MIG Welding", International Journal of Engineering Trends and Technology, Volume2, Issue2, 2011, PP: 28-33, ISSN: 2231-5381.
- [2]. A. Almazrouee, T. Shehata and S. Oraby "Effect of Welding Parameters on the Weld Bead Geometry of Low Alloy Steel using FCAW –Empirical Modeling Approach", International Journal of Mining, Metallurgy & Mechanical Engineering (IJMMME), Volume 3, Issue 3 (2015), PP: 88-92, ISSN 2320-4060.
- [3]. Sudhakaran. R, Sivasakthivel. P.S, Nagaraja.S and Eazhil. K.M "The Effect of Welding Process Parameters on Pitting Corrosion and Microstructure of Chromium manganese Stainless Steel Gas Tungsten Arc Welded Plates" 12thGlobal Congress on Manufacturing and Management, GCOMM 2014, PP: 790-800, ISBN: 978-1-63439-954-8 (Dec. 2014)
- [4]. T.A.Tabish, T.Abbas, M.Farhan, S.Atiq, T.Z.Butt, "Effect of heat input on microstructure and mechanical properties of the TIG welded joints of AISI 410 stainless steel" International Journal of Scientific & Engineering Research, Volume 5, Issue 7, July-2014, ISSN 2229-5518.
- [5]. Benjamin Joseph, D. Katherasan, P. Sathiyaa and C. V. Srinivasa Murthy, "Weld metal characterization of 316L (N) austenitic stainless steel by electron beam welding process" International Journal of Engineering, Science and Technology, Vol. 4, No. 2, 2012, pp. 169-176, ISSN: 2141-2820
- [6]. S. L. Jeng, H. T. Lee, T. E. Weirich and W. P. Rebach, "Microstructural Study of the Dissimilar Joints of Alloy 690 and SUS 410L Stainless Steel", Materials Transactions, The Japan Institute of Metals, Vol. 48, No. 3 (2007) pp. 481 to 489.
- [7]. Jun Yan, Ming Gao, Xiaoyan Zen "Study on microstructure and mechanical properties of 410 stainless steel joints by TIG, laser and laser-TIG hybrid welding", Elsevier, Optics and Lasers in Engineering, Vol. 48 (2010), PP: 512-517
- [8]. Radha Raman Mishra, Visnu Kumar Tiwari, "A Study of Tensile Strength of MIG and TIG Welded Dissimilar Joints of Mild Steel And Stainless Steel", International Journal of Advances In Materials Science And Engineering (IJAMSE), Vol.3, No.2, April 2014
- [9]. K.Monika, M.BalaChennaiah, Dr.P.Nanda Kumar, "The Effect of Heat input on the Mechanical Properties of MIG Welded Dissimilar Joints", International Journal of Engineering Research & Technology (IJERT), ISSN: 2278-0181 Vol. 2 Issue 9, September – 2013.
- [10]. Raveendra A, Dr.B.V.R.Ravi Kumar, "Influence of Welding Parameters on Weld Characteristics of 5052 Aluminium Alloy sheet Using TIG Welding", International Journal of Application or Innovation in Engineering & Management (IJAIEM), Volume 3, Issue 3, March 2014 ISSN 2319 - 4847